УДК 539.128.2; 51-7: 539.074.3

OPTIMIZATION OF THE SET-UP FOR THE INVESTIGATION OF THE LIGHT-NUCLEI SPIN STRUCTURE AT THE INTERNAL TARGET OF THE NUCLOTRON

V. P. Ladygin [a], *S. Nedev* [b1]

[a] Joint Institute for Nuclear Research, Dubna

[b] University of Chemical Technology and Metallurgy, Sofia

The simulation of dp elastic scattering and dp breakup at intermediate energies has been performed. The parameters of the set-up for the internal target at the Nuclotron are optimized.

Выполнено моделирование процессов dp-упругого рассеяния и dp-развала при промежуточных энергиях. Оптимизированы параметры установки на внутренней мишени нуклотрона.

INTRODUCTION

A new generation of nucleon–nucleon (NN) potentials describes the existing NN data up to the pion threshold production with a high accuracy. Therefore, the preference among different NN-interaction models cannot be established from this NN-data base. The quality of various NN-interaction models can be tested in the presence of additional nucleons, for example, in 3-nucleon ($3N$) systems. The development of rigorous techniques for solving the Faddeev equations for the $3N$ system enables one to compare the predictions of different NN-interaction models with experimental data at a new level of accuracy. On the other hand, the nuclear medium renormalization effects, parametrized in the form of a $3N$ potential, can be exactly included in the calculations, too.

Already in elastic Nd scattering there are significant discrepancies between the measured observables and the theoretical predictions based on pure NN potentials [1]. Even the differential cross section [2, 3] cannot be explained in the framework of the Faddeev approach without considering 3-nucleon forces ($3NF$) when all 3 nucleons are involved in the interaction [4,5]. The agreement between the calculations with $3NF$ [4] and the measured analyzing powers is not so good. For instance, the inclusion of $3NF$ improves an agreement of the calculations only for the vector analyzing power A_y, but at the same time, such calculations conflict with the data on the tensor analyzing powers A_{yy} and A_{xx} [3]. The investigations of deuteron breakup in the selected kinematical configurations can also provide substantial effects which can be used to test the $3N$ dynamics. The differential cross section and vector analyzing power A_y in the ^{2}H($\mathbf{p}$, pp)n reaction, obtained in complanar geometry, show a

[1] e-mail: nedev@uctm.edu

significant discrepancy with the Faddeev calculation even with the inclusion of the $3NF$ effect [6]. Such discrepancies can be even more dramatic in noncomplanar geometry and, especially, in the so-called space star configuration when all 3 nucleons are emitted in directions separated by $120°$ in the c. m. [7]. The reason of this may be a nonadequate description of the spin-dependent part of the $3NF$.

The main idea of the LNS project is the extension of the measurements of different observables in the processes involving 3-nucleon systems in a new energy and angular domain where the Faddeev technique is still working, and hence the comparison of experiment and theory can be made at a high level of accuracy.

The measurements of the cross section, vector A_y, tensor A_{yy} and A_{xx} analyzing powers in dp elastic scattering and dp breakup reactions up to a 500 MeV deuteron kinetic energy are proposed for the internal target at the Nuclotron. The goal of this work is to optimize the parameters of the set-up for such investigations.

1. SHORT DESCRIPTION OF THE SET-UP

The measurements of the observables in dp elastic scattering and deuteron breakup reactions will be performed using an internal target station [8] at the Nuclotron. A schematic view of the set-up is shown in Fig. 1. The CH_2 target up to 10 μm in thickness will be used. The intensity will be monitored by detecting pp quasi-elastic scattering in the vertical plane. The systematic error in the absolute normalization of the cross section is expected to be 3–5 %.

Elastic events will be detected by four pairs of detectors, each of them detects the proton and the deuteron in coincidence. The pairs will be placed symmetrically in the directions of azimuthal angles at left, right, up, and down (see Fig. 1). The analyzing powers A_y and A_{yy}

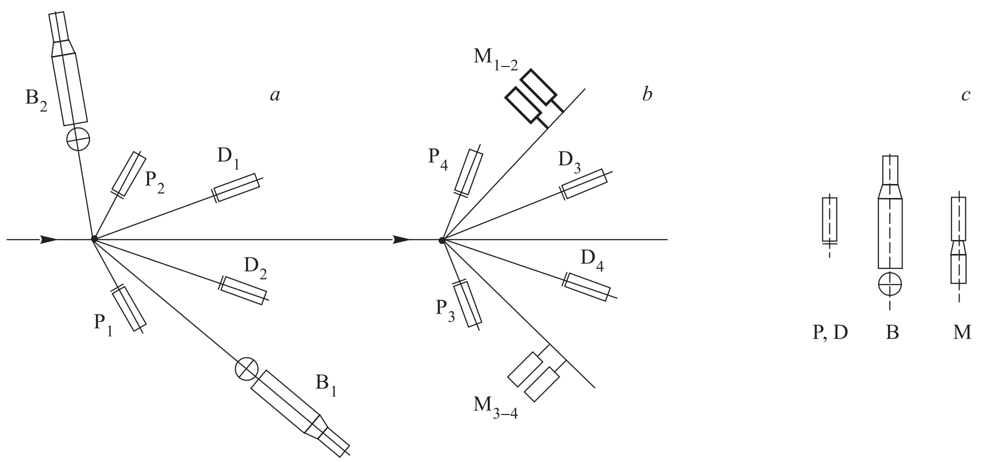

Fig. 1. The schematic view of the internal target experiment: P_i and D_i are the proton and deuteron detectors; B_i — $\Delta E - E$ detectors; M_i — monitor counters. *a*) Horizontal plane; *b*) vertical plane; *c*) schematic view of P, D, B and M detectors

can be extracted from the counts of the left and right pairs of detectors, while A_{xx} can be obtained from the counts of the up and down pairs.

Beam polarization will be measured by low-energy polarimeters and by this set-up at 270 MeV, where precise data exist [3]. The systematic error due to polarization measurement is expected to be 4–5 %.

The dp breakup reaction will be investigated in another experiment using $\Delta E - E$ techniques for the detection of protons. One of the detectors consists of 2 scintillation counters: the first one with a thin scintillator (1 cm) and the second with 20 cm in length. The diameter of the E-counter scintillator is 10 cm. Useful events will be selected by the time of flight difference and $\Delta E - E$ information for the detected particles.

2. dp ELASTIC SCATTERING

The proposed detector consists of two arms with scintillator counters at the ends (see Fig. 2). Lead degraders can be placed in front of the scintillators to stop the particles with low energies and to maximize energy losses in the scintillator. The purpose of one arm is to detect deuterons, another arm detects protons from dp elastic scattering. They are called the deuteron and proton arms. Each detector consists of a plastic scintillator 1–2 cm in thickness coupled to the photomultiplier tube. The radius of the cylindrical scintillator is 1 cm. The distances of the proton and deuteron detectors from the target are 50 and 70 cm, respectively. The angle acceptance of the two-arm device in the centre-of-mass system is $\pm 2.4°$.

The purpose of the experiment is to measure the tensor analyzing powers A_{yy} and A_{xx} up to a deuteron kinetic energy of 500 MeV at different deuteron scattering angles between 60° and 140° in the centre of mass. Monte-Carlo simulation has been performed for an energy of 500 MeV at two different deuteron scattering angles of 60° and 120° in the centre of mass. The corresponding kinematic variables are given in Table 1. The goal of the simulation is to optimize the thicknesses of the scintillators and degraders, to estimate the background for different configurations and to find the selection criteria for dp elastic events.

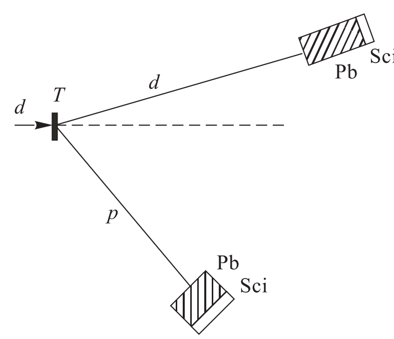

Fig. 2. Layout of the two-arm detector for the dp elastic-scattering experiment: T is the target; Sci are the scintillators; Pb are the lead degraders

For a scintillator thickness of 2 cm, the optimum thickness of the proton (deuteron) degrader is 1.33 cm (8.24 cm) and 10.34 cm (1.56 cm) at 60° and 120° deuteron scattering angles, respectively. Such thicknesses are necessary to maximize the energy losses of particles in the scintillator for better selection of dp elastic events and to eliminate the background coming from deuteron disintegration with three nucleons in the final state, $dp \to ppn$, when two protons are detected by the two arms.

Simulations with 2- and 3-particle phase space for the set-up without degraders give the ratios of elastic-to-breakup events $\sim$ 950 at 60° and $\sim$ 800 for the triggered, i. e., simultaneously detected particles in the two arms. If we accept the $1/5$ ratio of the elastic-to-breakup

Table 1. **Kinematics for dp elastic scattering at 500 MeV and 60° and 120° deuteron scattering angles in the c. m.**

$\theta_p^{\text{c. m}}$	θ_p^{lab}	T_p, MeV	$\theta_d^{\text{c. m}}$	θ_d^{lab}	T_d, MeV
60	27.41	337.8	120	29.98	162.2
120	57.26	112.6	60	18.32	387.4

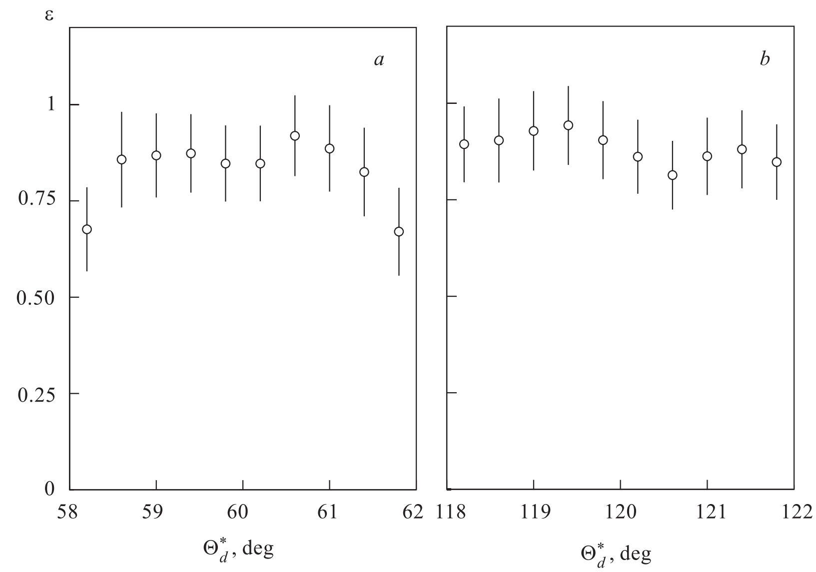

Fig. 3. Efficiency of the dp elastic-events detection versus deuteron scattering angle in c. m. in the case of lead degrader thickness for proton arm of 1.33 cm (*a*) and for deuteron arm of 1.56 cm (*b*)

cross section [9], the expected noise-to-signal ratio is 0.52 % at 60° and 0.62 % at 120°, respectively.

The efficiency of the elastic-events detection decreases with the using of the degraders. For example, the efficiency is 0.20 and 0.66 at 120° and 60° deuteron scattering angles, respectively. However, in this case, the background from deuteron breakup is completely eliminated. The detection efficiency decreases to ~ 0.9 using only one degrader either for the proton at 60° or for the deuteron at 120° (see Fig. 3, *a*, *b*, respectively). However, in this case the number of breakup events decreases by 70 % and 20 % only.

The energy losses and times of flight (TOF) of the proton and deuteron from dp elastic scattering are strictly correlated. This correlation is distorted by the dispersion of energy losses and instrumental resolution. The protons from breakup are not so strictly correlated, and this difference between these two kinds of interactions can be used to decrease the background additionally.

The correlation of the energy losses of two detected particles in the scintillators 2 cm thick at 500 MeV for two kinematics is shown in Fig. 4, *a*, *b*. The angles of the detectors correspond

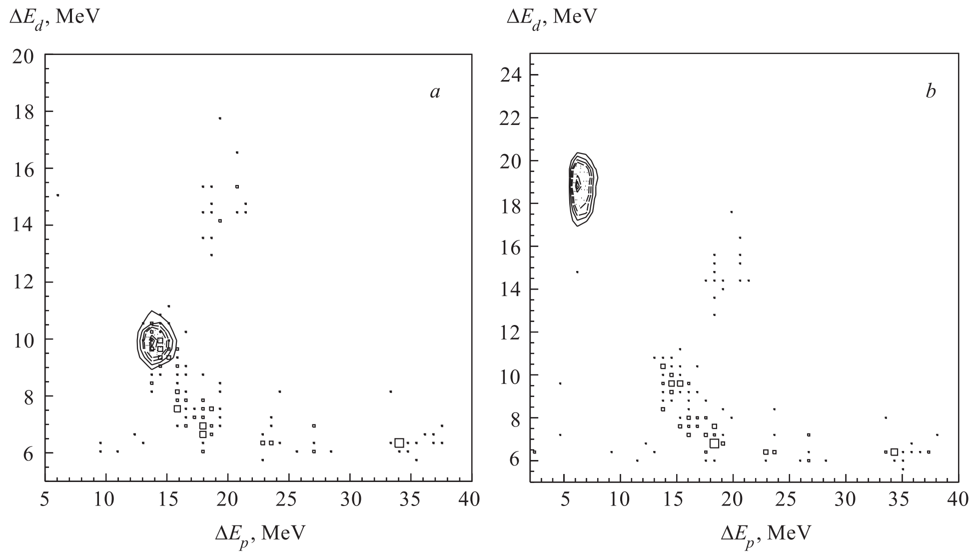

Fig. 4. Correlation of two detected-particles energy losses in 2 cm scintillators at 500 MeV and angles corresponding to the deuteron scattering angle of 60° (*a*) and 120° (*b*) in the c. m. The contour and boxes represent the events coming from dp elastic scattering and dp breakup, respectively

Table 2. **The efficiency of dp elastic breakup event selection using different criteria. The results are obtained at 500 MeV and detection angles corresponding to a 60° and 120° deuteron scattering angle in the c. m. without degraders**

60° cuts (energies in MeV)	Elastic, %	Breakup, %	120° cuts (energies in MeV)	Elastic, %	Breakup, %
$dE_p > 0$; $dE_d > 0$	100	0.52	$dE_p > 0$; $dE_d > 0$	100	0.62
$12 < dE_p < 17$ $8 < dE_d < 12$	93	0.14	$5 < dE_p < 8$ $16 < dE_d < 22$	92	0.03
$\lvert \mathrm{TOF}_p - \mathrm{TOF}_d$ $+0.456\rvert < 0.15$ ns	100	0.12	$\lvert \mathrm{TOF}_p - \mathrm{TOF}_d$ $+3.522\rvert < 0.15$ ns	99	—
TOF + dE	93	0.11	TOF + dE	91	—

to the cases of a deuteron scattering angle of 60° and 120° in the c. m., respectively (see Table 1). The contours and boxes show a correlation of energy losses of the deuteron and proton from dp elastic scattering and two protons from deuteron breakup, respectively.

The TOF and energy losses ΔE for the particle are correlated, but their uncertainties are not; therefore, both TOF and ΔE cuts can be used during off-line analysis. The results of Monte-Carlo simulation given in Table 2 show that the application of the criteria of energy losses in the scintillators and of TOF difference for both detected particles provides the selection of elastic events with an efficiency of higher than 90 %. On the other hand, the breakup events are completely eliminated at 120° and are $\sim 0.1\,\%$ only at 60°. The use of a 1 cm scintillator thickness gives approximately the same efficiency of dp elastic-event registration (with the corresponding degrader). However, the selection of dp elastic events without using degraders will be more complicated because the energy losses of particles are at least twice as small as in the case of a 2 cm scintillator.

The use of lead degraders, energy losses and time-of-flight cuts provides a significant suppression of breakup background with a high efficiency of dp elastic-event detection.

3. $dp \to ppn$ REACTION

Deuteron breakup, $dp \to ppn$, will be investigated by measuring the energies of both protons. Two counters with 1 and 20 cm scintillators will be used to measure energy losses and total energy, respectively. The opening angle of each detector is $\pm\,2^\circ$ in the laboratory frame.

Monte-Carlo simulation has been performed at a 500 MeV initial deuteron energy and at $\pm\,40^\circ$ proton emission angles in accordance with 3-particle phase space. The energy losses of the proton in the 1 cm, ΔE_1 (multiplying by factor 5), and 20 cm, ΔE_2, scintillators versus the energy of the detected proton are shown in Fig. 5, *a*. One can see that the proton energy between $\sim$ 20 and $\sim$ 100 MeV depends on the energy losses in the thick scintillator ΔE_2 uniquely, but at higher values this dependence becomes double branched. In this region, the energy losses in the two scintillators must be used simultaneously to obtain the proton energy, but the error in the calculated energy in this case is larger. In order to avoid this, simulation was made with a 1.5 cm lead degrader placed between the two scintillators. As

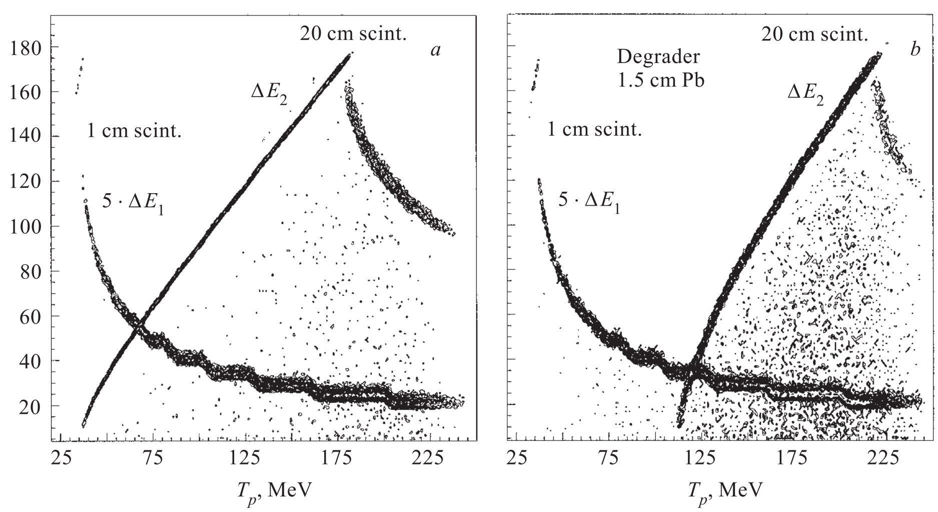

Fig. 5. Energy losses of proton in 1 and 20 cm scintillators, respectively. The lead degrader 1.5 cm thick is placed in front of the 20 cm scintillator (*b*)

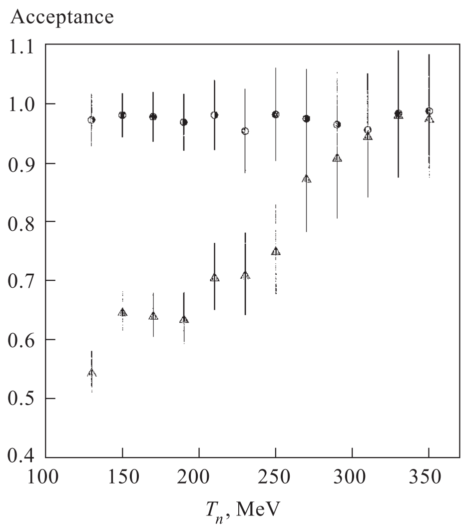

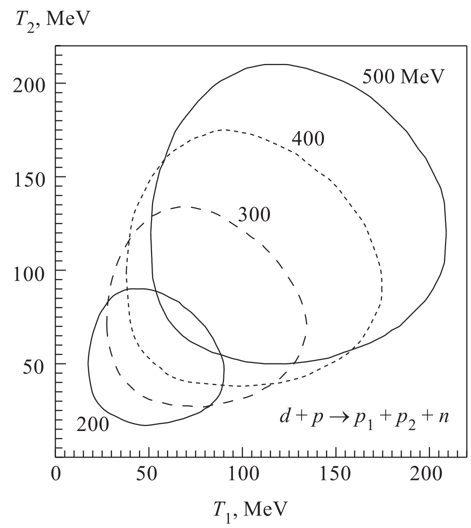

Fig. 6. Acceptance of the set-up for the case, when both protons are emitted at $\pm\ 40^\circ$ in the complanar geometry at a deuteron kinetic energy of 500 MeV versus energy of undetected neutron. Circles and triangles are obtained without and with the use of 1.5 cm Pb degrader, respectively

Fig. 7. Kinematic loci for the $dp \to ppn$ reaction, when both protons are emitted at $\pm\ 40^\circ$ in the complanar geometry at different initial energies

can be seen from Fig. 5, *b*, two branches are shifted closer to the kinematic limit. But in this case the energy losses ΔE_1 must be used to calculate the proton energy at energies lower than 110 MeV.

The acceptances versus neutron energy for the two cases are plotted in Fig. 6. They are calculated as a ratio between the reconstructed events, when two protons are triggered simultaneously, and all the events. It is seen that the efficiency in the case of degrader decreases by a factor of 2 at low energy. However, the use of the degrader allows one to extend the energy range of proton detection up to ~ 230 MeV. Figure 7 shows the kinematic loci for the $dp \to ppn$ reaction when both protons are emitted at $\pm 40^\circ$ for different deuteron energies. One can see that the measurements at energies between 200 and 400 MeV can be performed without a degrader. At higher energies, it is necessary either to increase the thickness of the scintillator or to use the lead degrader.

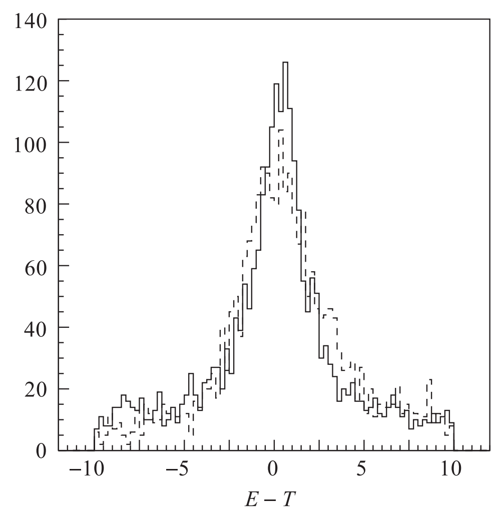

Fig. 8. The difference between the real and reconstructed energies of undetected neutron in the $dp \to ppn$ reaction at 500 MeV and at $\pm\ 40^\circ$ proton emission angles. The solid and dashed lines are obtained without and with 1.5 cm Pb degrader, respectively

The difference between the real and reconstructed energies of undetected neutron in the $dp \to ppn$ reaction at 500 MeV and at $\pm 40°$ proton emission angles is shown in Fig. 8. The reconstructed energy is obtained from the energies of the two detected protons. The solid and dashed lines are obtained for the cases without and with a 1.5 cm Pb degrader, respectively. One can see that the energy resolution of the set-up for both cases is practically the same.

CONCLUSIONS

The results of Monte-Carlo simulation show that the use of a 2 cm thick scintillator is more preferable than the use of a 1 cm one for the detection of dp elastic scattering.

The use of degraders allows one to eliminate the breakup background, however, it reduces significantly the detection efficiency of dp elastic events.

Using the correlation of energy losses and TOF difference for both detected particles, events selection provides a good separation of elastic events from the deuteron breakup background.

In this respect, the use of information on the energy losses of particles and timing information, as well as the installation of degraders, could help to optimize the efficiency of elastic event selection and background suppression.

It is shown that the use of $\Delta E - E$ techniques for the investigation of the $dp \to ppn$ reaction allows one to cover an initial deuteron energy range between 200 and 500 MeV in specific kinematics. It is better not to use a degrader between the two scintillators because in this case the acceptance of the set-up at low proton energies decreases and the energy resolution is worse.On the other hand, the use of the lead degrader allows one to increase the energy range of the measured proton. Therefore, such a method can be used in the region where the acceptance of the set-up is high.

The authors would like to express their thanks to the members of LNS project and especially to Yu. S. Anisimov, Prof. A. I. Malakhov, Prof. V. N. Penev and S. G. Reznikov for their permanent support. One of the authors (S. N.) thanks the LHE JINR for the kind hospitality where part of this work has been performed.

REFERENCES

1. *Glöckle W. et al.* // Phys. Rep. 1996. V. 274. P. 107.
2. *Shimizu H. et al.* // Nucl. Phys. A. 1982. V. 382. P. 242;
   Chamberlain O., Stern M. O. // Phys. Rev. 1954. V. 94. P. 666;
   Sagara K. et al. // Phys. Rev. C. 1994. V. 50. P. 576.
3. *Sakamoto N. et al.* // Phys. Lett. B. 1996. V. 367. P. 60.
4. *Witala et al.* // Phys. Rev. Lett. 1998. V. 81. P. 1183.
5. *Nemoto S. et al.* // Phys. Rev. C. 1998. V. 58. P. 2599.
6. *Bieber R. et al.* // Nucl. Phys. A. 2001. V. 684. P. 536c.

7. *Howell C. R. et al.* // Nucl. Phys. A. 1998. V. 631. P. 692;
Rauprich G. et al. // Nucl. Phys. A. 1991. V. 535. P. 313;
Strate J. et al. // Nucl. Phys. A. 1989. V. 501. P. 51;
Zejma J. et al. // Phys. Rev. C. V. 55. P. 42.
8. *Malakhov A. I. et al.* // Nucl. Instr. Meth. 2000. V. 440. P. 320.
9. *Katayama N. et al.* // Nucl. Phys. A. 1985. V. 438. P. 685.

Received on March 4, 2002.